ANL/ET/CP-95453

DEVELOPMENT AND APPLICATION OF NDE METHODS FOR MONOLITHIC AND CONTINUOUS FIBER CERAMIC MATRIX COMPOSITES*

W. A. Ellingson, J. G. Sun, T. A. K. Pillai,** and G. A. Forster
Energy Technology Division
Argonne National Laboratory
Argonne, IL 60439

** University of Wisconsin, LaCrosse

May 1998

INVITED PAPER submitted to the 9th International Conference on Modern Materials & Technologies/World Ceramics Congress & Forum on New Materials, Florence, Italy, June 14-19, 1998

*Research supported by the U.S. Department of Energy, Office of Industrial Technologies/ Materials Program, and Office of Transportation Systems/Heavy Vehicle Technologies Program, under Contract W-31-109-ENG-38.

DISCLAIMER

DEVELOPMENT AND APPLICATION OF NDE METHODS FOR MONOLITHIC AND CONTINUOUS FIBER CERAMIC MATRIX COMPOSITES*

W. A. Ellingson, J. G. Sun, T. A. K. Pillai,† and G. A. Forster

Energy Technology Division
Argonne National Laboratory, Argonne, IL 60439

†University of Wisconsin, LaCrosse

Monolithic structural ceramics and continuous fiber ceramic matrix composites (CMCs) are being developed for application in many thermally and chemically aggressive environments where structural reliability is paramount. We have recently developed advanced nondestructive evaluation (NDE) methods that can detect distributed "defects" such as density gradients and machining-induced damage in monolithic materials, as well as delaminations, porosity, and throughwall cracks, in CMC materials. These advanced NDE methods utilize (a) high-resolution, high-sensitivity thermal imaging; (b) high-resolution X-ray imaging; (c) laser-based elastic optical scattering; (d) acoustic resonance; (e) air-coupled ultrasonic methods; and (f) high-sensitivity fluorescent penetrant technology. This paper discusses the development and application of these NDE methods relative to ceramic processing and ceramic components used in large-scale industrial gas turbines and hot gas filters for gas stream particulate cleanup.

INTRODUCTION

Advanced structural ceramics, including monolithic materials, Si_3N_4, and SiC, as well as continuous fiber ceramic composites (CMCs) such as $SiC_{(f)}/SiC$, $Al_2O_{3(f)}/Al_2O_3$, are being extensively studied for applications such as combustor liners for low-emission gas turbines and heat exchangers, and hot-gas filters for fossil energy systems. While initial performance of these materials can be estimated from extensive laboratory data, there is a need to ensure the quality of as-produced preservice components and to establish part status once in service. Nondestructive evaluation (NDE) methods can provide data on component status. In the case of monolithic materials, critical flaws (e.g., a crack) can be quite small (50-100 μm for a rotating blade in a gas turbine); see Fig. 1.

* Research supported by the U.S. Department of Energy, Office of Industrial Technologies/Materials Program and Office of Transportation Systems/Heavy Vehicle Technologies Program.

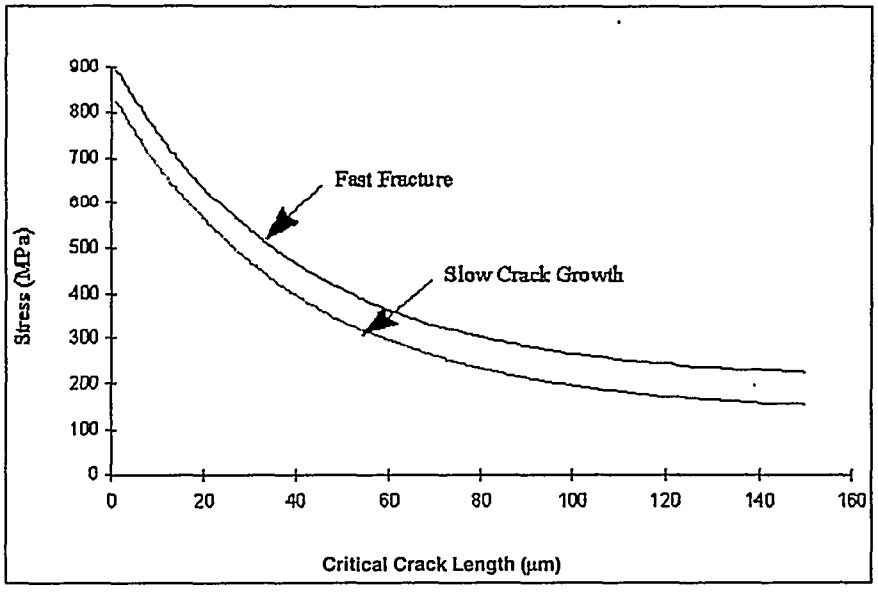

Fig. 1. Typical critical crack lengths for rotating turbine blade of monolithic Si_3N_4

Critical flaw sizes for CMCs are more difficult to predict because of limited material data bases. It thus becomes almost necessary for NDE data to be used to measure more globally distributed changes in the material. "Defects," from an NDE viewpoint, more closely resemble a distributed property to be determined. Such distributed properties may be thermal (such as thermal diffusivity) or physical (such as density and elastic modulus). While 3-D weave geometries are used for some CMCs, they have not been extensively developed and no results are presented here for these fiber lay-ups. 2-D lay-ups are more common and require NDE data to detect interlaminar delaminations, as well as through-thickness density, because of the different methods used for infiltrating the 2-D lay-ups. NDE methods that have been developed for these CMC materials include thermal imaging for diffusivity measurements, air-coupled ultrasonics for detecting delamination defects, and X-ray computed tomography (XCT) for determining density variations, primarily through the walls of cylindrical specimens. The following sections will discuss aspects of these NDE methods, and examples of applications will be given.

NDE DEVELOPMENT FOR MONOLITHIC CERAMICS

We have devoted a significant effort to the development of NDE methods for monolithic materials; detection sensitivities were reported in Refs. 1-3. Two NDE methods will be described here and examples given of applications.

(a) Dye Penetrant

We recently reevaluated dye penetrants (4-6) because of concerns about detection sensitivity. In our work, a set of specially prepared specimens of Si_3N_4 and SiC were used with a surface roughness range of 0.046 - 0.186 μm, Ra. A Vickers microhardness indentor was used to generate of controlled cracks; the Vickers loads ranged from 5 to 20 kg.

Crack length data were acquired by measuring the length of the detected crack across the indent as well as the optical indent diagonal indent. Several indents were made on each test specimen so that independent penetrant data were acquired from each specimen. An optical microscope was retrofitted with a mercury light and appropriate filters to allow only UV radiation to pass through the optical system; no special optical components were used. This microscope allowed a range of magnifications from 40 to 400 X. Images were acquired through a digital low-light CCD array camera and archived in a computer. Typical test results are shown in Fig. 2, which contains both an optical microscope image and a dye penetrant image.

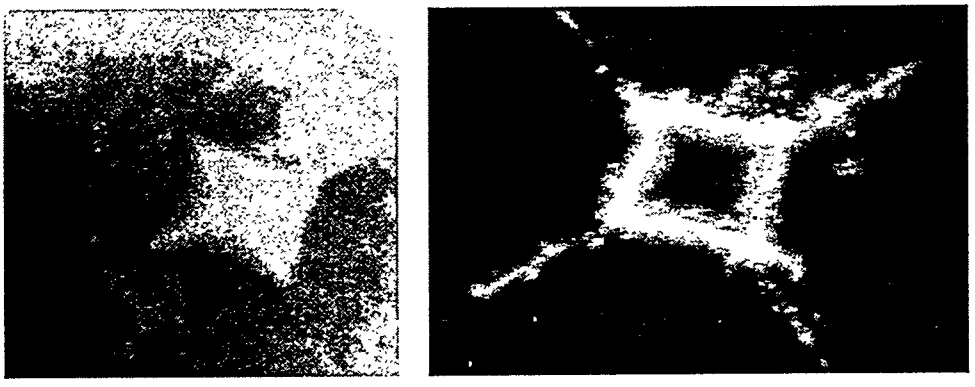

(a) (b)

Fig. 2. Dye penetrant image data: (a) optical photomicrograph of Vickers indent, (b) typical dye penetrant image of same specimen.

The penetrant approaches included in this study included capillary gaseous diffusion (7), fluorescent dye (5,6), and visible dye. After analysis, we concluded that 40-60X magnification was sufficient to establish crack length and that fluorescent dyes are the most appropriate for monolithic ceramics. Recent work by Domon et al. (4) has suggested that the proper light intensity for such application is 1500 $\mu W/cm^2$.

(b) Elastic Optical Scattering

Details of the optical scattering NDE method were reported in Ref. 8. In this approach, a specimen is directly illuminated by a focused laser beam, and the amount and distribution of backscattered light is monitored. For subsurface analysis, the basic material requirement is that the specimens have partial translucency at the optical wavelength available, e.g., 0.6328 μm.

The optical system in this method utilizes two detectors and beam-focusing optics, as shown in Fig. 3. The backscattered light that passes through the surface-illuminating polarized beam splitter (PBS) is incident on a second PBS. Light passing the first PBS then passes through a λ/4 plate, is focused onto a stainless steel pinhole aperture ≈100 μm in diameter, and is recorded by Detector A. The remaining light that is scattered from the area is imaged by a positive lens onto Detector B, and also by a video camera to monitor the scattering surface.

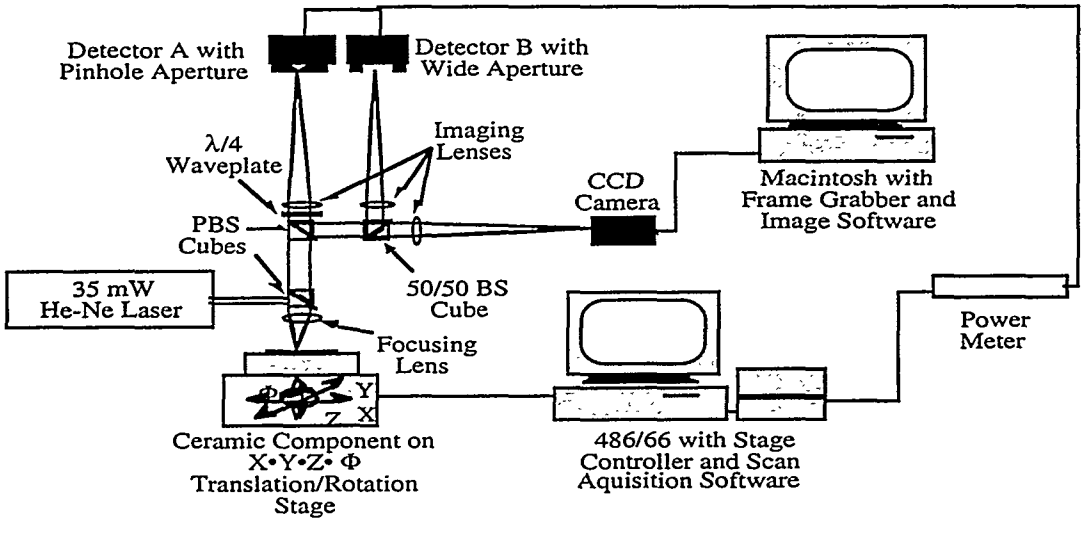

Fig. 3. Schematic diagram of two-detector laser scattering system

By monitoring the sum of the outputs of Detectors A and B, i.e., A + B, we can measure the total backscattered intensity. It has been demonstrated that this sum will be most indicative of lateral defects. The ratio of outputs from Detectors B and A, i.e., B/A, is an indication of the degree of lateral subsurface cracks. As the laser illumination is rastered across the specimen surface, these values are assembled into a gray-scale "image."

Optical transmittance as a function of thickness has been measured for several different Si_3N_4 ceramics at a wavelength of 0.6328 μm (He-Ne laser); results were reported in Ref. 8.

The sensitivity of the laser scattering technique to Hertzian cracks has been demonstrated. For this work, an array of Hertzian cracks (see Fig. 4) was generated in a flat 4-mm-thick plate of NBD-200 Si_3N_4. Three cracks, for each surface diameter of ≈925 μm, ≈540 μm, and ≈410 μm, as well as a "C-crack," were generated. Laser scattering images were obtained by using sum data. The resulting 200-μm-step scans are shown in Figs. 4b and c. Although the surface scan reveals all of the cracks, only the C-crack is visible when the optical system is set for subsurface scan. This is shown more clearly in Fig. 5, which shows a magnified view of the C-crack at a spatial resolution of 20 μm.

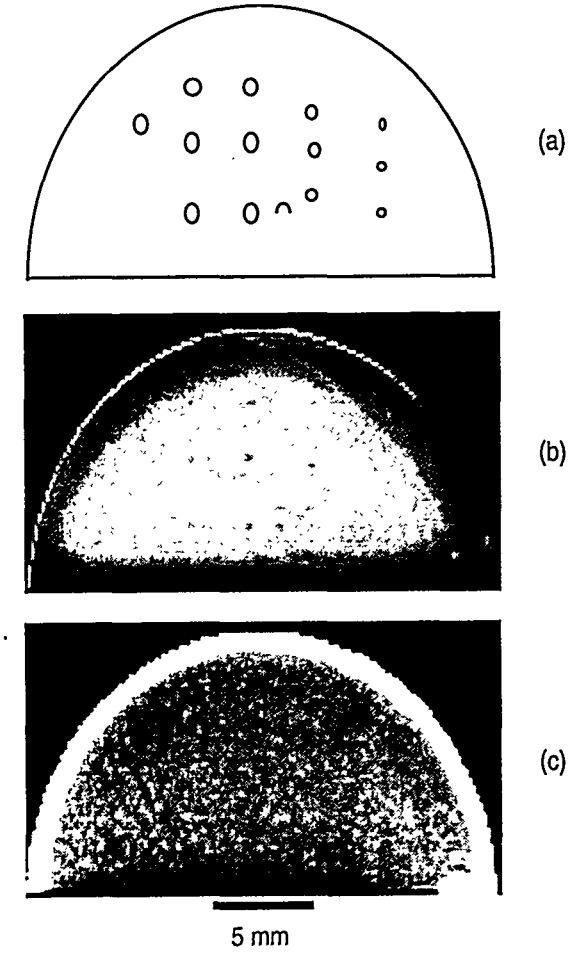

Fig. 4
Locations and relative sizes of Hertzian cracks and C-crack in an NBD-200 specimen: (a) schematic representation, (b) surface laser scattering scan, and (c) subsurface laser scattering scan.

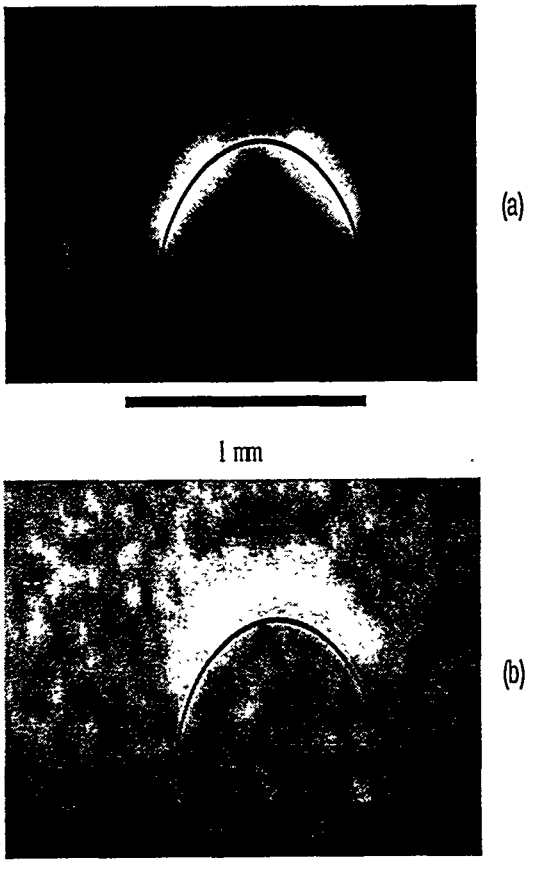

Fig. 5
Magnified view of C-crack Fig. 4. (a) surface and (b) subsurface laser scattering images. Line drawing of surface-breaking crack is superimposed.

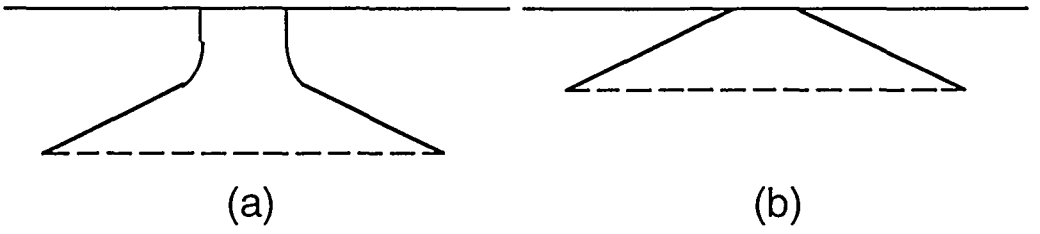

Fig. 6. Cross-sectional representation of (a) Hertzian crack and (b) C-crack.

This sensitivity to the different Hertzian cracks can be explained by Fig. 6. The surface-breaking C-crack extends laterally directly from the surface, whereas the Hertzian crack first extends in a cylindrical fashion normal to the surface before turning and extending laterally. If the depth of the cylindrical portion of the Hertzian crack is greater than the penetration depth of the laser, no signal scatter will be detected. Thus, because the penetration depth into NBD-200 has been measured as ≈150 μm, we can assume that the Hertzian cracks shown in Fig. 4 are at least ≈150 μm below the surface. This technique has also been explored recently for detecting creep in Si_3N_4. Results are presented in Ref. 9.

NDE DEVELOPMENT FOR COMPOSITE CERAMICS

CMCs are being developed for application to combustors in natural-gas-fired industrial gas turbine engines, high-temperature heat exchangers, and hot-gas filters for coal gasification systems. These material systems include SiC(f)/SiC, Al_2O_3(f)/SiC, and Al_2O_3(f)/Al_2O_3. CMC material systems offer many advantages, including noncatastrophic failure and high fracture toughness at elevated temperature (>1250°C). For reliable operation, these applications require that uniform thermal properties be ensured both prior to installation of the component and during the lifetime of the component. Development of NDE methods that can measure uniform thermal properties, e.g., diffusivity, is thus of prime importance. Nondestructive techniques based on infrared thermographic imaging have been developed to characterize the uniformity of thermal properties. Presently, there is concern about water contamination in SiC-based materials produced by several processes and thus the traditional water-coupled ultrasonic methods would not be useful. For this reason, air-coupled ultrasonic (ACUT) methods (10) have been under study.

Because complex curvatures may be difficult to evaluate with either ACUT or thermal methods, X-ray computed tomographic imaging has also been developed primarily to detect throughwall density variations and delaminations. Two NDE methods under development will be described and application examples given.

(a) Air-Coupled Ultrasonic System

The experimental setup of our air-coupled ultrasonic system consists of a traditional xyz positioning system with two matched 400 kHz air-coupled transducers in a coaxial transmission geometry, as shown in Fig. 7.

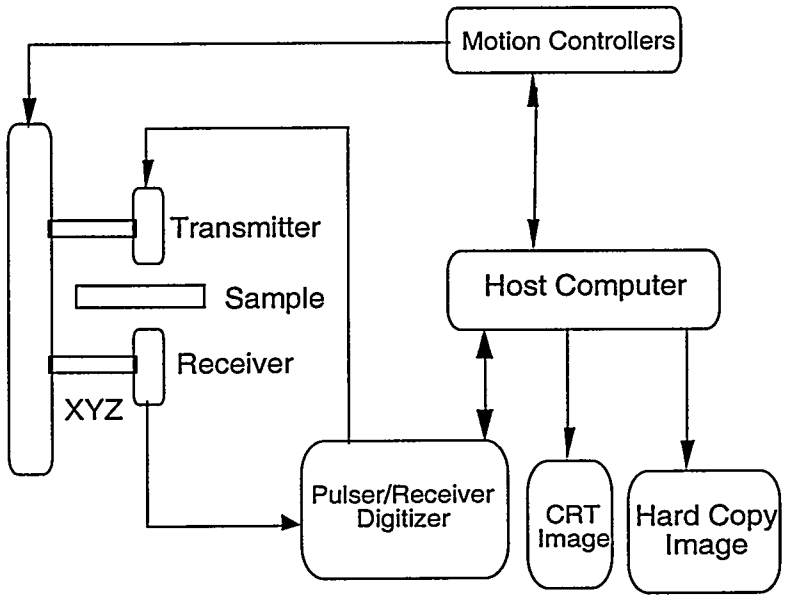

Fig. 7. Schematic diagram of air-coupled ultrasonic system.

While there may be several air-coupled transducer configurations including electrostatic, piezoelectric, variable reluctance, moving coils, electrostrictive, and magnetostrictive, all data reported here are based on 400 kHz piezoelectric, air-backed, focused transducers.

The yoke assembly on which the transducers are mounted is connected to xy scan stepper motors that are controlled by the host computer. The sample is mounted on an adjustable support so that the focal point of the transducers is within the thickness of the sample. A C-scan image of the sample is then built up with nominal 800 μm step size in both x and y directions. The detected signal is preamplified by a low-noise pre-amp attached directly to the receiving transducer. The data are acquired with a gated peak detector and stored as an 8-bit image.

(b) Thermal-Imaging System

The experimental system developed for measuring through-thickness thermal diffusivity has been described previously (11) and is shown in Fig. 8. The apparatus includes a focal-plane array 256 x 256 InSb detector IR camera with 12 bit dynamic range, a 200 MHz Pentium-based PC

equipped with locally written software, a frame grabber, a 6.4 kJ flash lamp system for the thermal impulse, a function generator to operate the camera, and a dual-timing-trigger circuit for the camera and external trigger control. An analog video system monitors the experiments.

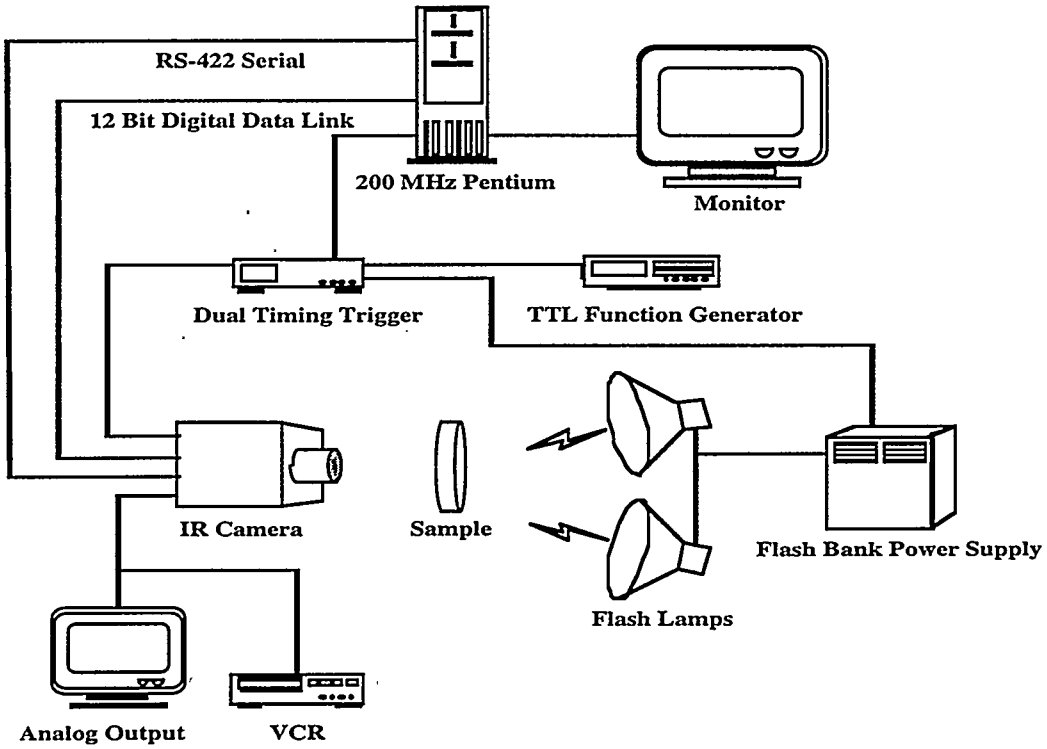

Fig. 8. Schematic diagram of experimental thermal imaging apparatus

The thermal diffusivity for through-wall calculations is based on the theory of Parker et al. (12) and assumes that the front surface of the sample is heated instantaneously. The rate of heat conduction through the sample is determined by measuring the temperature rise at the back surface. Thermal diffusivity measurements in this work have been based on the "half-rise-time" ($t_{1/2}$) method (11) in which the measured back-surface temperature is used, and on the relation $\alpha = 1.37L^2/\pi^2 t_{1/2}$, where α is diffusivity, L is specimen thickness, and t is time.

More recently, because of the need to obtain data on specimens with one-sided access, the infrared system has been modified to allow the camera and thermal pulse to be mounted on the same side of the specimen.

EXAMPLES OF APPLICATIONS

Two examples will be given here. One for a cylindrical oxide/oxide combustor liner, and the second is for a square flat plate specimen.

A 20-cm-diameter $Al_2O_{3(f)}/Al_2O_3$ liner with a 3-mm-thick wall was examined for defects. Both thermal imaging and ACUT were used. Figure 9 shows both an infrared diffusivity image map and a through-transmission C-scan air-coupled ultrasonic image for this liner. The black regions suggested a delaminated region and the grey "stripe" suggests a fabric overlap with likely low infiltration. Subsequent destruction analysis verified the delamination.

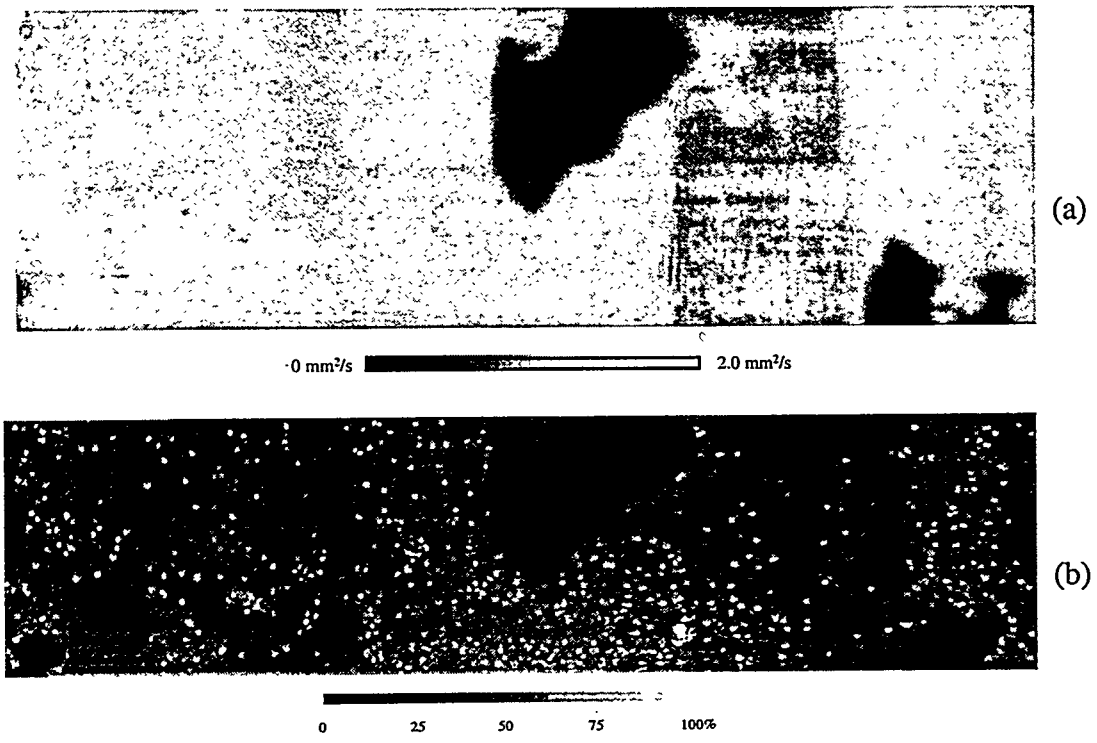

Fig. 9. NDE image data for 20-cm-diam $Al_2O_{3(f)}/Al_2O_3$ cylinder: (a) thermal diffusivity image and (b) air-coupled C-scan ultrasonic image.

(b) Flat Plates for Process Development

A second example used a $SiC_{(f)}/SiC$ 2-D lay-up set containing an 8-ply panel formed by polymer impregnation processing (PIP) using cyclic deposition. The panel measured 203 x 203 mm, and thermal imaging and air-coupled NDE tests were conducted after 1, 5, 10, and 15 PIP cycles.

NDE data clearly showed several regions of damage in the panel, and subsequent analysis verified that the damage was in a form of delamination.

An attempt was made to estimate bulk density from thermal diffusivity image data, as shown in Fig. 10. Although the trends between the measured and estimated densities are the same, the estimated values exaggerate the variation. However, this problem is expected because the

correlation was obtained from uniform composite materials, whereas the measured density variation in the sample was due to a delamination.

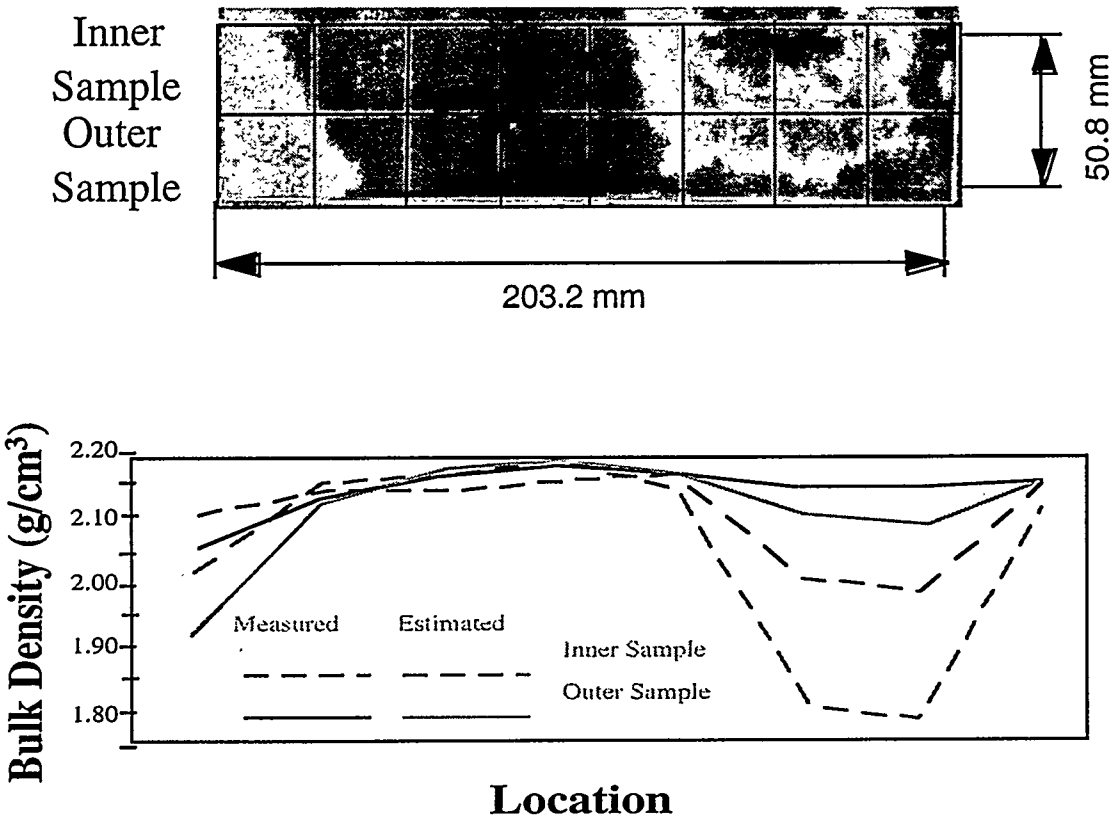

Fig. 10. Measured and estimated bulk density of 51 x 203-mm 8-ply SiC/SiC, CMC composite sample.

CONCLUSIONS

NDE methods currently under development for monolithic and composite ceramics show promise for detecting damage to in-service components and for improving ceramic processing. NDE data acquired by these new methods must now be closely coupled to lifetime prediction models that incorporate NDE data as a primary input.

REFERENCES

1. Y. IKEDA, Y. MIZUTA, K. ONDA, H. DOMON and T. UDAGAWA, "NDE of Fine Ceramics with Ultrasonic and Its Reference Test Pieces," to be published in Proc. of the Ceramics and Composites Conf., Cocoa Beach, FL, 1998.

2. Y. IKEDA, Y. MIZUTA and K. ONDA, "NDE of Fine Ceramic with X-ray and Its Reference Test Pieces," ibid.

3. Y. IKEDA, Y. MIZUTA, H. TOBITA and H. USAMI, "X-ray CT Test for Parts and Materials of Ceramic Gas Turbines," in Proc. 1995 Yokohama Int. Gas Turbine Cong. III, pp. 29-36.

4. H. DOMON, K. UEMURA and K. FUJIWARA, "Liquid Penetrant Test for Fine Ceramics," Proc. 8th Asia-Pacific Conf. on NDT, Taipei, Taiwan, 1995, pp. 711-718.

5. S. A. HORTON, "Detection of Surface Defects in Ceramic Rolling Elements," in 4th Int. Symp. on Ceramic Materials and Components for Engines, June 1991, Göteborg, Sweden, pp. 897-904.

6. R. J. MALINS, D. MCCALL and G. W. RHODES, "Systems Level Considerations for Environmentally Responsive Fluorescent Penetrant Testing," Mat. Eval. Vol. 51, No. 3, 338-352, Mar. 1993.

7. N. G. BERIOZKINA, M. N. LARICHEV, I. O. LEIPUNSKY, G. L. EREMIN and N. M. DERGUNOV, "Indicator Capillary-Diffusion Method for Nondestructive Defectoscopy of Composite Materials," in Proc. Moscow Int. Composites Conf. (MICC), Nov. 14-16, 1990, Moscow, Elsevier Science, UK (1991), pp. 773-776.

8. J. S. STECKENRIDER and W. A. ELLINGSON, "Application of Laser Scattering to the Detection of Surface and Subsurface Defects in Si_3N_4 Components," Cer. Eng. and Sci. Proc., Vol. 15, No. 4, pp. 382-389, 1994.

9. J. A. TODD, A. WOLOSEWICZ, J. G. SUN and W. A. ELLINGSON, "Detection of Damage in Crept Si_3N_4-$6Y_2O_3$-ZAl_2O_3 Using Elastic Optical Scattering" (see these proceedings).

10. T. A. K. PILLAI, W. A. ELLINGSON, J. G. SUN, T. E. EASLER and A. SZWEDA, 1997, "A Correlation of Air-Coupled Ultrasonic and Thermal Diffusivity Data for CFCC Materials," in Ceramic Engineering & Science Proc., pp. 251-258, Vol. 18, No. 4.

11. J. G. SUN, C. DEEMER, W. A. ELLINGSON, T. E. EASLER, A. SZWEDA and P. A. CRAIG, 1997, "Thermal Imaging Measurement and Correlation of Thermal Diffusivity in Continuous Fiber Ceramic Composites," presented at 24th Int. Thermal Conductivity Conf., Pittsburgh, Oct. 26-29, 1997.

12. W. J. PARKER, R. J. JENKINS, C. P. BUTLER and G. L. ABBOTT, "Flash Method of Determining Thermal Diffusivity, Heat Capacity, and Thermal Conductivity," J. Appl. Phys., 32:1679-1684, 1961.